



UvA-DARE (Digital Academic Repository)

Coherent X-ray scattering of charge order dynamics and phase separation in titanates

Shi, B.

Publication date

2017

Document Version

Other version

License

Other

[Link to publication](#)

Citation for published version (APA):

Shi, B. (2017). *Coherent X-ray scattering of charge order dynamics and phase separation in titanates*. [Thesis, fully internal, Universiteit van Amsterdam].

General rights

It is not permitted to download or to forward/distribute the text or part of it without the consent of the author(s) and/or copyright holder(s), other than for strictly personal, individual use, unless the work is under an open content license (like Creative Commons).

Disclaimer/Complaints regulations

If you believe that digital publication of certain material infringes any of your rights or (privacy) interests, please let the Library know, stating your reasons. In case of a legitimate complaint, the Library will make the material inaccessible and/or remove it from the website. Please Ask the Library: <https://uba.uva.nl/en/contact>, or a letter to: Library of the University of Amsterdam, Secretariat, Singel 425, 1012 WP Amsterdam, The Netherlands. You will be contacted as soon as possible.

Appendix C

Characterization of the coherent properties of the XCS beam line

In this appendix, we discuss various properties of the XCS beamline at the LCLS. The first section introduces the three operation modes used in our LCLS experiments: *continuous*, *burst* and *one shot* or often referred as *single shot*. We then characterize the longitudinal coherence of each mode by analyzing the intensity probability distribution function. Finally, we check these results by analyzing the photon statistics on the CCD detector.

C.1 Electron bunch and types of operation

The compressed electron bunch has a typical duration of ~ 80 fs, corresponding to a physical bunch-length of $25 \mu\text{m}$. The bunch profile, shown in the top panel of Fig. C.1 has peaks at the head and the tail of the bunch respectively. In the undulator, the SASE process causes the bunch to break up into micro-bunches which each emit coherent X-rays with a typical duration of 300 attoseconds, resulting in an X-ray pulse train with a length equal to that of the electron bunch. Due to the stochastic nature of the SASE process, these pulses vary in intensity by several orders of magnitude (see bottom panel of Fig. C.1). In the hard X-ray range, this results in a spiked single bunch spectrum with a FWHM of about 0.2 % or 16 eV at 8 keV. For this reason the raw undulator beam is called the *pink* beam. The LCLS data acquisition system records the electron energy and its corresponding pink beam energy for each pulse.

LCLS can be operated in continuous, burst and one shot mode, all of which were used in our experiment [108]. Examples of the recorded electron beam pulse energies are shown in Fig. C.2 for all three modes. In continuous mode, the machine runs at the maximum 120 Hz

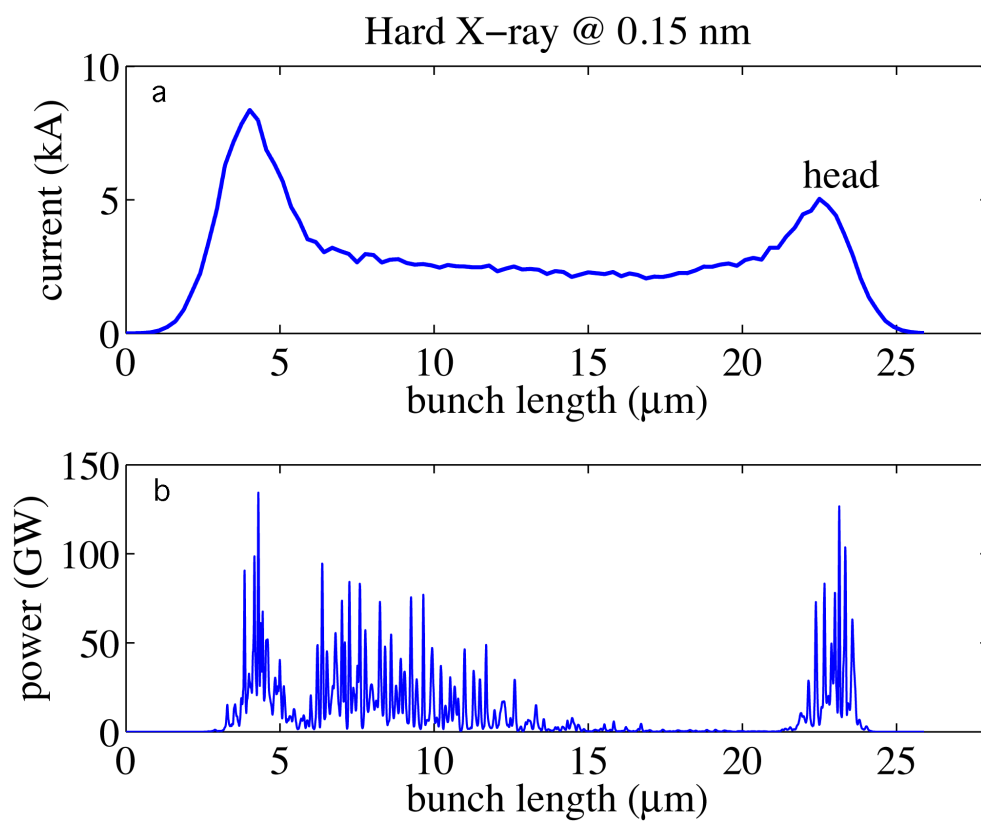


Fig. C.1 (a) The current profile of a compressed electron bunch with 250 pC charge. (b) The power profile of the resulting X-ray pulse train. Taken from LCLS FAQ web page [25].

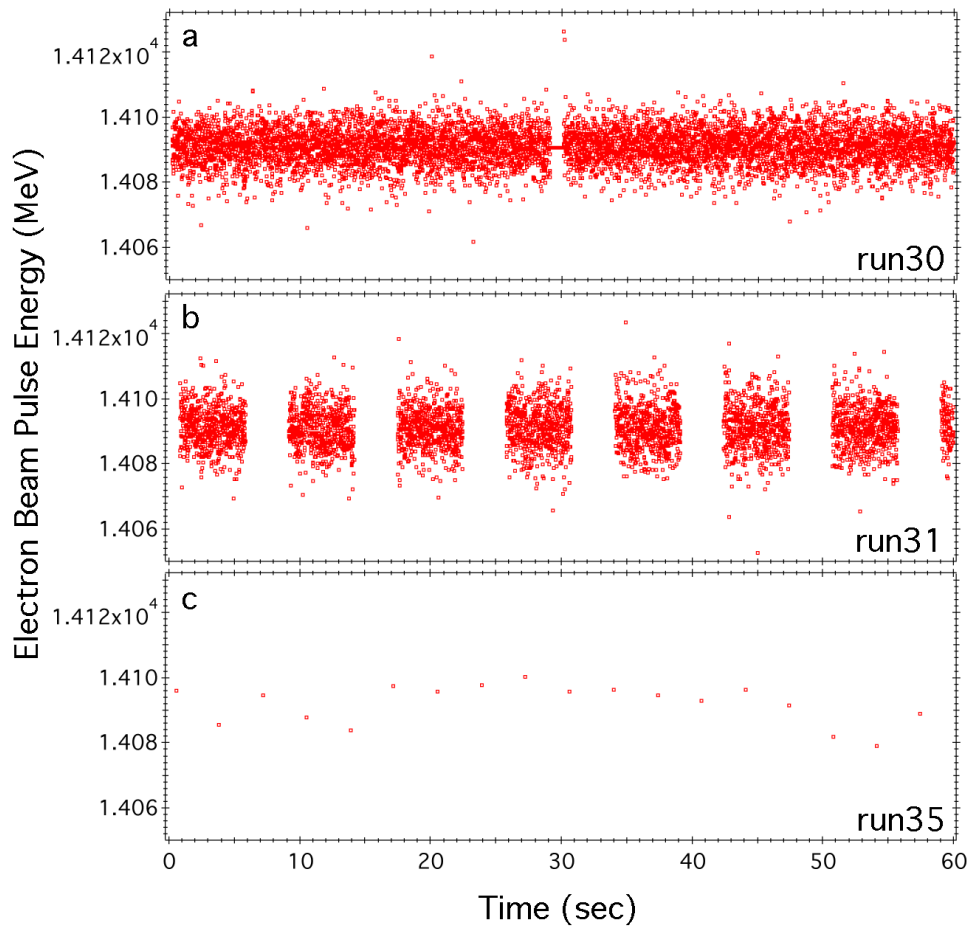


Fig. C.2 Examples of the electron beam pulse energy for the three LINAC operation modes used in our experiments: (a) 120 Hz continuous mode, (b) burst mode, (c) one shot mode. The nominal energy of the electron beam pulse energy is 14091 MeV

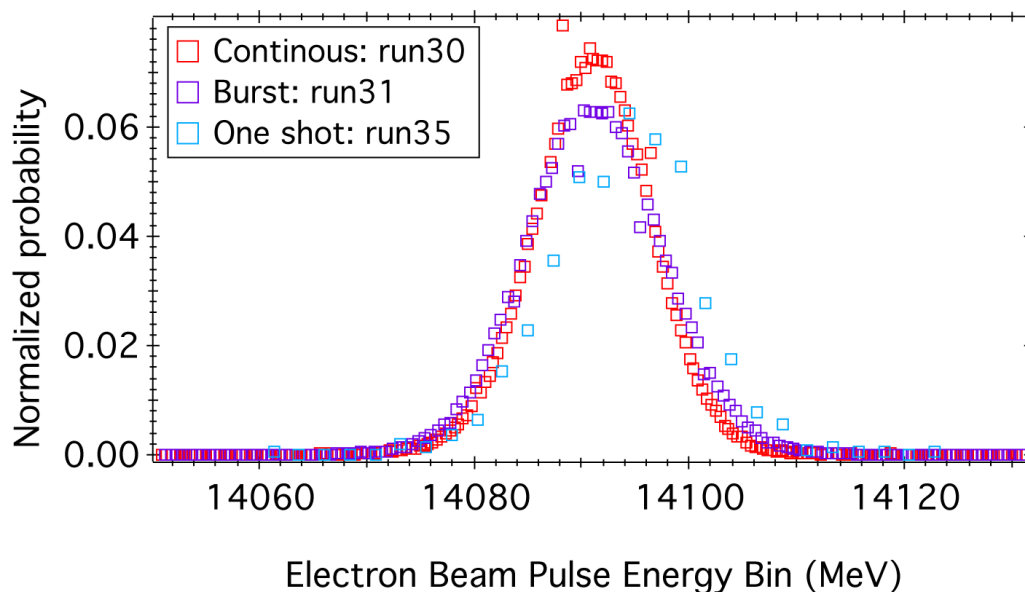


Fig. C.3 Energy distribution of the electron beam modes shown in Fig. C.2.

repetition rate. It requires a detector that can handle the equal amount of frame rate, such as the Timepix detector. In bunch mode, a user-determined number of pulses is emitted, allowing one to integrate the signal of the pulses on a conventional CCD detector with a long readout time. In single shot mode, one can record a single 80 fs shot with a rather flexible time interval between consecutive shots.

Fig. C.3 shows the electron beam pulse energy distribution for each of the datasets in Fig. C.2. In each case the distribution is roughly Gaussian, centred at 14091 MeV with a FWHM of 8 MeV, although the one shot mode had a slightly higher nominal energy at 14904 MeV. Fig. C.4 (a) shows that the pink X-ray pulse energy and the electron beam pulse energy are fairly well correlated, although some electron pulses failed to lase properly.

The pink beam is monochromated by a four-crystal Si(011) monochromator with a bandwidth (FWHM) of 1.4 eV, *i.e.* 12 times smaller than the pink beam spectral width. As a result, a large number of X-ray pulses are partially or completely absorbed by the monochromator, and the resulting monochromatic beam energy of the pulses varies in intensity over many orders of magnitude. Therefore it also correlates much less with the electron pulse energy, as can be seen in Fig. C.4 (b).

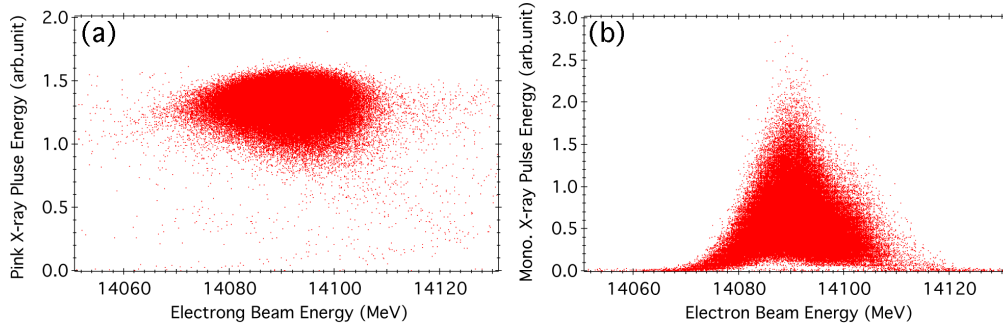


Fig. C.4 The correlation of the pink X-ray pulse energy(a) and the monochromatic X-ray pulse energy (b) with the electron pulse energy.

C.2 Determination of the longitudinal coherence length from the statistics of the monochromatic X-ray pulse energy

In Fig. C.5 we show the normalized distributions of the monochromatic X-ray pulse energy for a one-minute pulse train in each of the three different operation modes. Due to the stochastic nature of the source, the monochromatic pulse train can be described as a speckle time series [98, 141]. According to Goodman [97], the probability density function of such a series is a Gamma distribution.

By fitting the histograms with a Gamma function for each of the three cases, we obtain the temporal mode factor M_t which represents the average number of longitudinal coherent modes in the X-ray pulse. We find that this number is around $M_t=131$ for the pink beam and 4.2 for the monochromatic beam for all three operation modes. As expected, the monochromator improves the longitudinal coherence length. By dividing the pulse length by the number of modes one obtains a longitudinal coherence length of $6 \mu m$.

We repeated this procedure for all the runs taken in three experimental shifts, and the results are given in Fig. C.6. We find that the number of coherent modes varies with shifts between 2 and 4.2.

C.3 Determination of speckle modes from single shot photon count statistics

In an alternative method of determining the coherence of the monochromatic beam the photon statistics of multiphoton events in each of the single shot frames can be considered

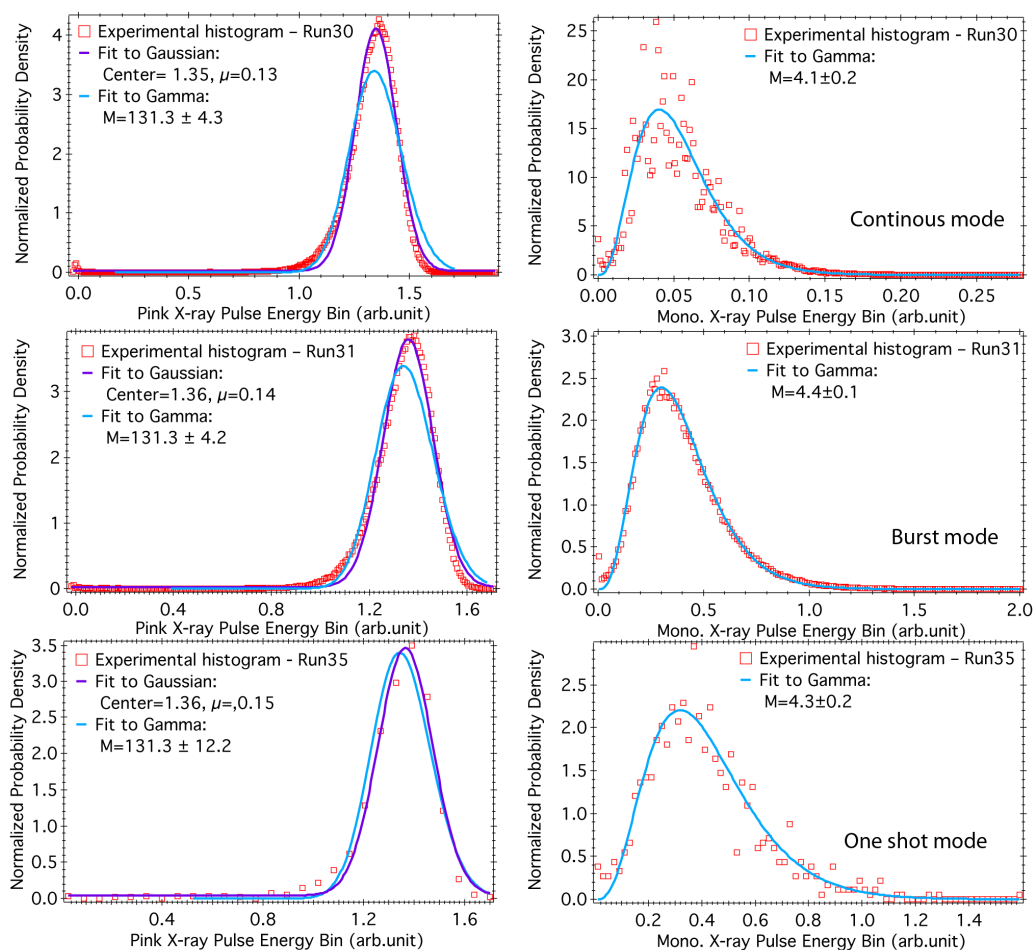


Fig. C.5 Distribution of the pink (left) and monochromatic X-ray pulse energy (right) for the continuous (top), burst (middle) and single shot (bottom) modes. The distributions are fitted with a Gamma function. For the pink distribution a Gaussian fit has also been included for comparison, as this is the limit of the Gamma function for high mode numbers.

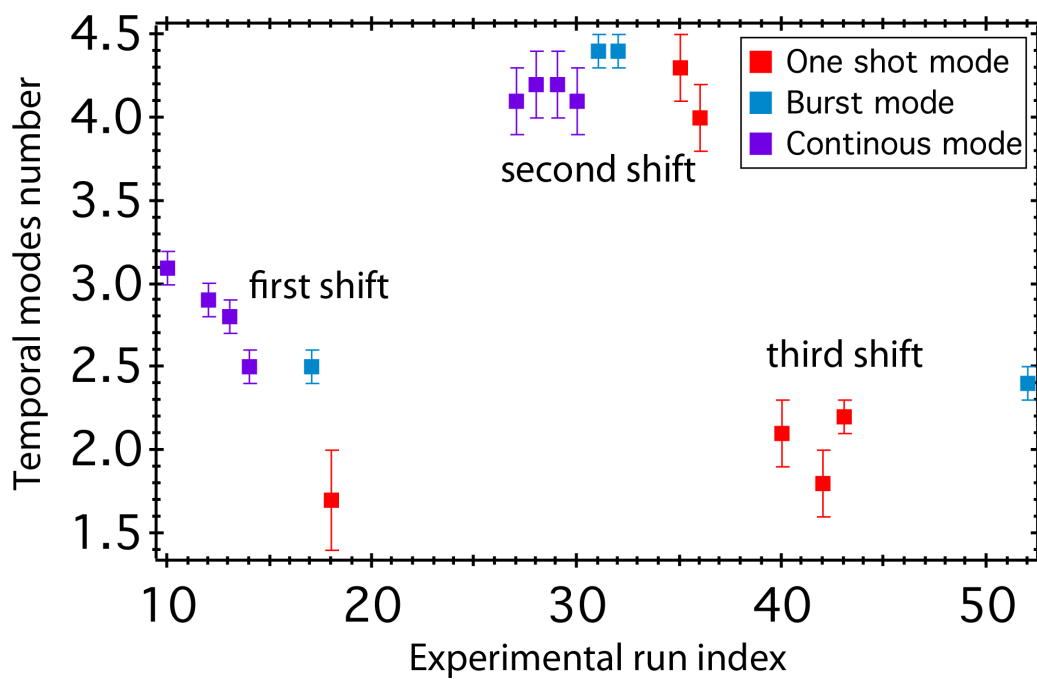


Fig. C.6 The number of longitudinal coherent modes in the monochromatic beam for all the runs in the three experimental shifts described here. A small run-to-run fluctuation in the mode number is observed, but the largest differences are between the shifts.

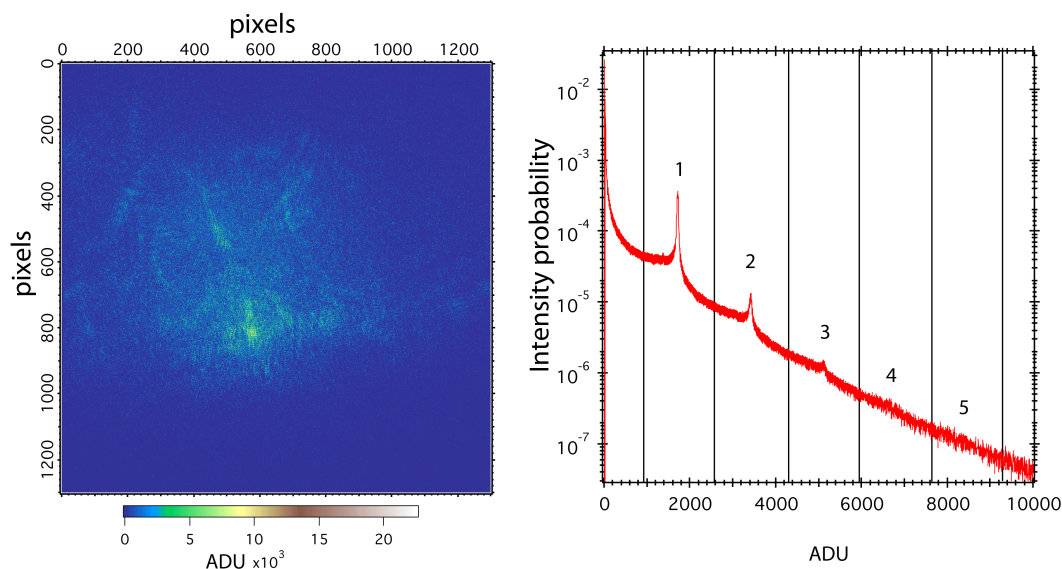


Fig. C.7 (a) A typical example of a single-shot Pixis frame (300 by 300 pixels from Run 18). (b) The intensity histogram on a log scale, obtained by summing the single shot histograms of all frames in the movie. The single and multi-photon peaks are visible. Vertical lines define the bins used to determine the number of photons per each pixel.

[98, 99, 142, 143]. We applied this method to single-shot movies of the (022) diffracted beam. In the single-shot Timepix data, the non-linearity of the photon response makes it difficult to determine precisely the number of photon events per pixel. However, two datasets were obtained in one shot mode using the Pixis detector, and these are suitable for this purpose. These movies were taken with a frame delay of 3.4 seconds at 168 K (run 18) and at 172 K (run 42), with a total movie length of 100 and 200 frames respectively.

To analyze these data, a dark current image (background) was subtracted from all frames. An example of the resulting single shot frames is given in Fig. C.7.a, where the color scale represents the photon energy in terms of Analogue to Digital units (ADU). Fig.C.7.b shows the cumulative histogram of the ADUs in the dataset. A number of sharp peaks can be distinguished, corresponding to 1, 2, 3 and 4 photon events that hit the same pixel in the one shot illumination mode. These peaks are broadened due to loss mechanisms in the detector and charge sharing between adjacent pixels. We determined the number of photons per pixel, k , in each single shot frame by binning according to the histogram, such that 850-2550 ADU counts corresponds to one photon, 2551-4250 counts to two, *etc.* (see the vertical lines in Fig.C.7 (b)). In addition, the average number of photons/pixel \bar{k} was determined for each frame. This number varies on a frame-by-frame basis by over 2 orders of magnitude, due to the intensity variation of the incoming light.

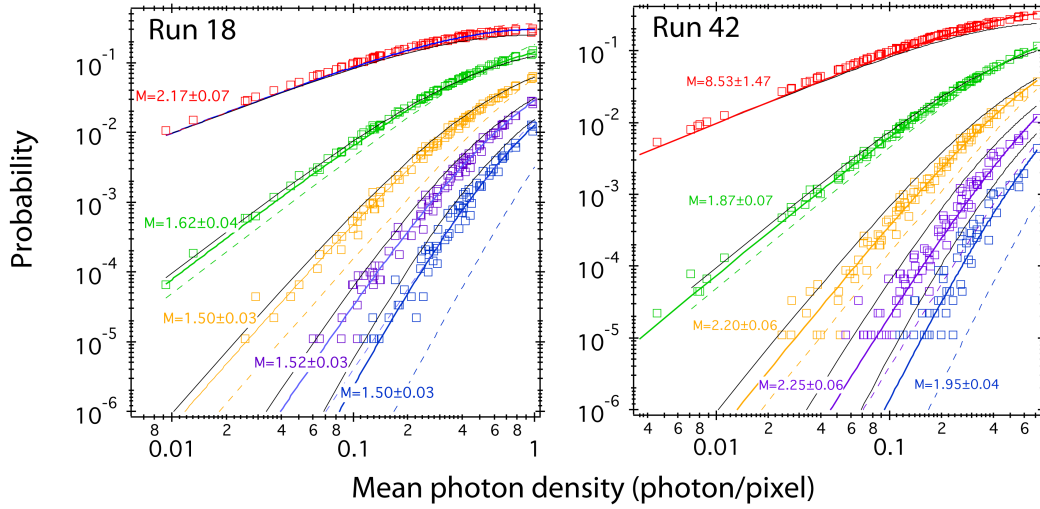


Fig. C.8 Experimental probability (colored squares) of having $k=1$ to 5 photons per pixels in a given single shot frame, plotted against the average number of photons per pixel of that frame \bar{k} . The thick colored lines are fits to these data with a negative binomial distribution function. The black lines indicate the $M=1$ curves. The dashed colored lines indicate the limiting case for $M=100$. Left: run 18, right run 42

In Fig. C.8, we plot the probability $P(k)$ of having $k=1, 2, 3, 4$ or 5 photons in a pixel versus \bar{k} for the two different datasets (run18 and run42). We fitted these curves with the negative binomial distribution function shown as Eq. 3.14 (colored solid lines), which applies to datasets with strongly fluctuating intensity [97–99]. For run 18, we find the number of coherent modes to be $M=1.5$ to 1.6, for all k except $k=1$ where M is 2.17, which could be due to a greater sensitivity of single photon effects to the details of the statistical procedure [99] and charge sharing effects. For run 42 we find $M=2$ to 2.2 for $k=2$ to 5. Again for $k=1$ the value, $M=8$, is much larger.

These values can be cross-checked to the mode numbers of the monochromatic beam before it was scattered by the sample, which according to Fig. C.6 were $M=1.8$ in both cases. This result is gratifying since it shows that two quite different approaches lead to the same conclusion, namely that within the X-ray pulse length the light beam contains two longitudinally coherent modes and that the scattering process does not reduce the longitudinal coherence.